WIND ENERGY
Wind Energ. 2013; **00**:1–12
DOI: 10.1002/we

RESEARCH ARTICLE

Model predictive control for wind power gradients

Tobias Gybel Hovgaard[1,3], Stephen Boyd[2] and John Bagterp Jørgensen[3]

[1]Vestas Technology R&D, Denmark. [2]Information Systems Laboratory, Department of Electrical Engineering, Stanford University, USA. [3]DTU Compute, Department of Applied Mathematics and Computer Science, Technical University of Denmark.

ABSTRACT

We consider the operation of a wind turbine and a connected local battery or other electrical storage device, taking into account varying wind speed, with the goal of maximizing the total energy generated while respecting limits on the time derivative (gradient) of power delivered to the grid. We use the turbine inertia as an additional energy storage device, by varying its speed over time, and coordinate the flows of energy to achieve the goal. The control variables are turbine pitch, generator torque, and charge/discharge rates for the storage device, each of which can be varied over given ranges. The system dynamics are quite nonlinear, and the constraints and objectives are not convex functions of the control inputs, so the resulting optimal control problem is difficult to solve globally. In this paper, we show that by a novel change of variables, which focuses on power flows, we can transform the problem to one with linear dynamics and convex constraints. Thus, the problem can be globally solved, using robust, fast solvers tailored for embedded control applications. We implement the optimal control problem in a receding horizon manner and provide extensive closed-loop tests with real wind data and modern wind forecasting methods. The simulation results using real wind data demonstrate the ability to reject the disturbances from fast changes in wind speed, ensuring certain power gradients, with an insignificant loss in energy production.

KEYWORDS

wind power ramps, electrical grid integration, disturbance rejection, model predictive control, convex optimization, wind power control, energy storage, power output optimization

Correspondence
Tobias Gybel Hovgaard, Vestas Technology R&D, Hedeager 42, DK-8200 Aarhus N, Denmark.
E-mail: togho@vestas.com

Received . . .

1. INTRODUCTION

Today, wind power is the most important renewable energy source. For the years to come, many countries have set goals for further reduction of CO_2 emission, increased utilization of renewable energy, and phase out of fossil fuels. In Denmark one of the means to achieve this is to increase the share of wind power to 50% of electricity consumption by 2020 (in 2012 this number was 30%) and to fully cover the energy supply by renewable energies in general by 2050 [1]. Installing this massive amount of wind turbine capacity introduces several challenges to reliable operation of power systems due to the fluctuating nature of wind power. Thus, modern wind power plants (WPP) are interfaced with power electronic converters that are required and designed to fulfill grid codes (see, *e.g.*[2, 3]).

The Grid Code (GC) is a technical document setting out the rules, responsibilities and procedures governing the operation, maintenance and development of the power system. It is a public document periodically updated with new requirements and it differs from operator to operator. Countries with large amounts of wind power have issued dedicated GCs for its connection to transmission and distribution levels, focused mainly on power controllability, power quality and fault ride-through capability [4, 5]. In general, wind power plants at transmission level shall act as close as possible to conventional power plants, providing a wide range of power output control based on transmission system operator (TSO) instructions. For instance, Denmark, Ireland and Britain establish some of the most demanding requirements regarding active power control [6]. One of the regulation functions required is a power gradient constraint that limits the maximum rate-of-change of non-commanded variations in the power output from the WPP to the grid. The reason for such grid codes

is that if large WPPs are allowed to produce power as the wind blows, other units on the grid must compensate for the power fluctuations. This can lead to very high power prices as well as stand in the way for phasing out the conventional power sources. As of today, this constraint is softened if the power production in the WPP drops due to the lack of wind. This is merely out of necessity and the GCs are expected to tighten further regarding this requirement. Ensuring slow power gradients reduces the risk of instability on the grid, allows the TSO time for counteracting the change, and improves the predictability of power output, enabling the WPP owner to put less conservative bids on the power market. In Europe, the ENTSO-E Network Codes for all types of Generators [7], published in June 2012, aims to establish a coherent set of non-discriminatory requirements applicable to all types of generators.

Energy storage addresses the major problems of wind power and joining energy storage with WPPs to smooth variations and improve the power quality is not a new idea. In, *e.g.*, [8, 9, 10, 11] the benefits, economics, and challenges of using different means of storage, *i.e.*, batteries, hydrogen, flywheels etc., in combination with wind power are investigated. [12] uses a Lithium-iron-phosphate battery to achieve power forecast improvement and output power gradient reduction. However, the additional cost of batteries or other energy storages is usually the showstopper, at least as the market is today. In our previous works, we have shown how thermal capacity, *e.g.*, in supermarket refrigeration, can be utilized for flexible power consumption [13, 14]. It is very likely that such techniques (where the capacity is a bi-product of fulfilling another need) can play a major role instead of adding expensive technologies which have storage as their sole purpose. In the rest of this paper, we consider energy storage in general without distinguishing actual storage from flexible power consumption.

Traditionally, the rotor speed of modern wind turbines is controlled such that it tracks the tip-speed ratio (TSR = angular rotor speed $\times$ rotor radius / wind speed) that extracts the maximum amount of power from the wind and is below the maximum allowed rotor speed. However, due to the inertia of the rotating masses in the turbine, there is a potential for improving the quality of the power output by actively letting the rotor speed deviate from the optimal setting. This might of course come at a cost of slightly reduced power output. In, *e.g.*, [15, 16] turbine inertia is used for frequency response and power oscillation damping. In these papers, the goal is to enable the wind turbines to offer ancillary services to the grid, whereas in this paper, we focus on maximizing the power output while observing strict grid codes. In addition, a vast amount of work exists that address power optimization, fatigue load reduction and pitch control for individual turbines in the more traditional sense, *e.g.*, [17, 18, 19, 20, 21]. Some of these take optimization and model predictive control approaches to solve the problems and many rely on a known operating point (*e.g.*, local wind speed and power set-point) for deriving linearized models. Other works consider the control of large wind farms where the power extracted by upwind turbines reduces the power that is available from the wind and increases the turbulence intensity in the wake reaching other turbines (see, *e.g.*, [22, 23, 24, 25, 26]).

The key contributions in this paper are: 1) A convex reformulation of the wind turbine model to a convex problem, 2) a fast solution algorithm for this problem, and 3) demonstration of the application by simulation using real wind speed data. We demonstrate how model predictive control (MPC) using forecasts of the wind speed can ensure very low power gradients (*e.g.*, less than 3% of the rated power per minute) to effectively limit the ramping up or down of power production even when such power ramps would be caused by sudden lack of wind speed. We do this with a central energy storage added to the WPP and show how we can utilize the inertia in the individual turbines to further improve this and minimize the extra storage capacity needed. In [27], we present a sequential convex programming approach to solve the optimal control problem for the same wind turbine problem as in this paper. The main novelties in this paper are the convex reformulation, the fast algorithm, and the demonstrations with real wind data, as mentioned above. During the last 30 years, MPC for constrained systems has emerged as one of the most successful methodologies for control of industrial processes [28, 29, 30]. Traditionally, MPC is designed using objective functions penalizing deviations from a given set-point. MPC based on economic performance functions that directly address minimization of the operational costs is an emerging methodology known as economic optimizing MPC [31, 32, 33, 34, 35]. The potential usefulness of Economic MPC has been demonstrated for a number of smart energy systems in, *e.g.*, [14, 36, 37]. Economic MPC addresses the concerns of controlling a system influenced by a number of disturbances which we can predict (with some uncertainty) over a time horizon into the future, obeying certain constraints, while minimizing the cost (or maximizing the profit) of operation. MPC is applied to wind turbine control in, *e.g.*, [38, 39] and in particular with focus on convex optimization in [40, 41]. [42, 43] consider convex optimization for a network of electrical devices, such as generators, fixed loads, deferrable loads, and storage devices. [44, 45, 46, 47] describe methods for improving the speed of MPC, using online optimization. These custom methods exploit the particular structure of the MPC. Embedded convex optimization applications have recently become more available to non-experts by the introduction of the automatic code generator CVXGEN [48]. Remarkable speed-ups achieved using tailored QP-solvers exported from CVXGEN have been reported in, *e.g.*, [42, 49] and in this paper, we use the same type of custom, embedded solvers. In a recent paper [50] a splitting technique to a generic linear-convex optimal control problem is introduced and computation times faster than what is obtained by CVXGEN are reported.

Wind Energ. 2013; **00**:1–12 © 2013 John Wiley & Sons, Ltd.
DOI: 10.1002/we
Prepared using weauth.cls

1.1. Outline

In §2, we introduce the dynamic model for a wind turbine along with the constraints from both physical/mechanical limitations and the constraints we impose in order to fulfill certain requirements to the operation. We specify and explain the individual terms in the composite objective function for the optimal control problem in §2.2. In §3, we show how the optimal control problem can be formulated as a convex optimal control problem, *i.e.*, one with linear dynamics convex constraints, and a concave objective functional (to be maximized). We provide a novel change of variables and justify the necessary approximations. §4 gives a numerical simulation of the open-loop optimization for a constructed scenario and we evaluate the performance of our proposed method. Finally, in §5, we propose an economic MPC based on the convex optimal control formulation and demonstrate the capability in closed-loop on three different scenarios with real wind measurement series and their corresponding forecasts using modern wind predictors. We give concluding remarks in §6.

2. SYSTEM MODEL

2.1. Dynamics and constraints

We model the turbine, transmission, and generator as a single rotational system, with generator speed $\omega_{\mathrm{g}}(t)$ in rad/s, and rotor speed $\omega_{\mathrm{r}}(t) = \omega_{\mathrm{g}}(t)/N$ in rad/s, where N is the gear ratio of the transmission. We let J_{g} and J_{r} denote the inertias of the generator and rotor, respectively, and we let $J = J_{\mathrm{g}} + J_{\mathrm{r}}/N^2$ denote the equivalent inertia at the generator shaft. Neglecting losses, the dynamics is given by

$$J\dot{\omega}_{\mathrm{g}}(t) = T_{\mathrm{r}}(t)/N - T_{\mathrm{g}}(t), \tag{1}$$

where $T_{\mathrm{g}}(t)$ is the generator (back) torque and $T_{\mathrm{r}}(t)$ is the rotor torque from the wind, in Nm. The generator speed and torque must lie within given bounds:

$$\omega_{\mathrm{g,min}} \leq \omega_{\mathrm{g}}(t) \leq \omega_{\mathrm{g,max}},$$
$$0 \leq T_{\mathrm{g}}(t) \leq T_{\mathrm{g,max}}.$$

The rotor torque $T_{\mathrm{r}}(t)$ is a function of rotor speed $\omega_{\mathrm{r}}(t)$, wind speed $v(t)$ (in m/s), and the blade pitch angle, denoted $\beta(t)$ (by convention in degrees), which must satisfy

$$\beta_{\min} \leq \beta(t) \leq \beta_{\max}.$$

The mechanical power extracted from the wind, denoted P_{w}, is

$$P_{\mathrm{w}}(t) = \omega_{\mathrm{r}}(t)T_{\mathrm{r}}(t) = \frac{1}{2}\rho A C_{\mathrm{P}}(v(t), \omega_{\mathrm{r}}(t), \beta(t))v(t)^3,$$

where ρ is the air density, A is the swept rotor area, and C_{P} is the coefficient of power, which is a function of wind speed, rotor speed, and blade pitch, typically given by a lookup table, found from aerodynamic simulations or tests. We write this in the form

$$T_{\mathrm{r}}(t) = \Phi(v(t), \omega_{\mathrm{r}}(t), \beta(t))v(t)^3/\omega_{\mathrm{r}}(t),$$

where we combine several terms into one function

$$\Phi(v(t), \omega_{\mathrm{r}}(t), \beta(t)) = (1/2)\rho A C_{\mathrm{P}}(v(t), \omega_{\mathrm{r}}(t), \beta(t)).$$

The generator produces power $P_{\mathrm{g}}(t)$, given by

$$P_{\mathrm{g}}(t) = \eta_{\mathrm{g}} T_{\mathrm{g}}(t)\omega_{\mathrm{g}}(t),$$

where $\eta_{\mathrm{g}} \in [0, 1]$ is the generator efficiency. This power is constrained by

$$P_{\min} \leq P_{\mathrm{g}}(t) \leq P_{\mathrm{rated}},$$

where P_{rated} is the rated power of the generator.

Let $Q(t)$ denote the state-of-charge of the energy storage device, in J. With a small charge and discharge loss, the dynamics of $Q(t)$ is

$$\dot{Q}(t) = P_{\mathrm{chg}}(t) - \eta_{\mathrm{loss}} \left| P_{\mathrm{chg}}(t) \right|, \tag{2}$$

where $P_{\mathrm{chg}}(t)$ is the charge rate, in W. (Negative $P_{\mathrm{chg}}(t)$ means decharging.) $\eta_{\mathrm{loss}} \in [0, 1]$ is the loss in per cent. Charge rate and state-of-charge are limited by

$$P_{\mathrm{chg,min}} \leq P_{\mathrm{chg}}(t) \leq P_{\mathrm{g}}(t),$$

and

$$0 \leq Q(t) \leq Q_{\max}.$$

The limits on state-of-charge are considered as logical charge levels, and need not correspond to actual charge levels of the battery: $Q(t) = 0$ simply means that the storage is at its minimum allowed charge state. Finally, the power supplied to the grid is

$$P_{\mathrm{grid}}(t) = P_{\mathrm{g}}(t) - P_{\mathrm{chg}}(t).$$

2.2. Optimization

We assume that the limits on quantities, data such as N and J, the function Φ (and therefore the functions $\omega_{\mathrm{r}}^{\star}$ and $\beta_{\mathrm{r}}^{\star}$), are known, along with the initial rotor speed and state of charge. We assume that the wind speed $v(t)$ is known (or estimated) over the time interval $0 \leq t \leq T$. Our goal is to choose the blade pitch $\beta(t)$, generator torque $T_{\mathrm{g}}(t)$, and charge rate $P_{\mathrm{chg}}(t)$, over the time interval $0 \leq t \leq T$, subject to all the constraints described above.

We have several objectives to consider. The first is the total energy E over the period,

$$E = \int_0^T P_{\mathrm{grid}}(t)\, dt,$$

which we want to maximize. The second is a penalty (which we wish to minimize) for violating a target maximum value of power rate of change, G (in W/s):

$$R_{\mathrm{pen}} = \int_0^T (|\dot{P}_{\mathrm{grid}}(t)| - G)_+\, dt,$$

where $(b)_+ = \max(b, 0)$. The third objective, which we want to minimize, is a measure of variation of delivered power over time:

$$R_{\mathrm{var}} = \int_0^T \dot{P}_{\mathrm{grid}}(t)^2\, dt.$$

The forth objective is a penalty (which we will minimize) on rotational speeds above the rated speed $\omega_{\mathrm{g,rated}}$:

$$R_{\mathrm{speed}} = \int_0^T (\omega_{\mathrm{g}}(t) - \omega_{\mathrm{g,rated}})_+\, dt,$$

so over-speed is limited when it is not needed for storing kinetic energy. Finally, the fifth objective is to reduce the generator torque by increasing rotational speed to the rated speed when more power is available in the wind than what the generator is able to extract. This is achieved by maximizing

$$R_{\Phi} = \int_0^T \Phi(v(t), \omega_{\mathrm{r}}(t), \beta(t))\, dt.$$

We handle these objectives by maximizing the composite objective

$$E - \lambda R_{\mathrm{pen}} - \mu R_{\mathrm{var}} - \rho R_{\mathrm{speed}} + \gamma R_{\Phi},$$

where λ, μ, ρ, and γ are positive constants that determine the tradeoffs among the objectives. We are to choose $\beta(t)$, $T_{\mathrm{g}}(t)$, and $P_{\mathrm{chg}}(t)$ to maximize the composite objective, subject to the constraints given above, and the final charge constraint $Q(T) = Q(0)$, which says that the net energy from the storage device over the period is zero.

This is a classical continuous-time optimal control problem, with nonlinear dynamics and nonlinear objective functional.

3. CONVEX FORMULATION

In this section, we show how the optimal control problem described above can be formulated as a convex optimal control problem, *i.e.*, one with linear dynamics, convex constraints, and a concave objective functional (to be maximized). This implies that the problem can be solved globally, with great efficiency and also great reliability [51].

Wind Energ. 2013; **00**:1–12 © 2013 John Wiley & Sons, Ltd.
DOI: 10.1002/we
Prepared using weauth.cls

The trick is to work with power flows and energies, treating $\beta(t)$ and $T_{\rm g}(t)$ as variables derived from the powers. In our formulation we choose the quantities

$$P_{\rm g}(t), \quad P_{\rm grid}(t), \quad P_{\rm chg}(t), \quad P_{\rm w}(t), \quad Q(t), \quad K(t),$$

over the time interval $0 \leq t \leq T$, where $K(t) = (J/2)\omega_{\rm g}(t)^2$ is the kinetic energy stored in the rotational motion and $P_{\rm w}(t) = T_{\rm r}(t)\omega_{\rm r}(t)$ is the power extracted from the wind. Note that the rotor speed can be expressed in terms of the kinetic energy as

$$\omega_{\rm r}(t) = (1/N)\sqrt{(2/J)K(t)}$$

(which shows how we reconstruct it from the variables above).

The objective E is a linear function of the variables, hence concave. The minimization objectives $R_{\rm pen}$ and $R_{\rm var}$ are convex functions of the variables, and $R_{\rm speed}$ translates directly to:

$$R_{\rm speed} = \int_0^T (K(t) - (J/2)\omega_{\rm g,rated}^2)_+ \, dt,$$

which is a convex function of K. So the over all objective $E - \lambda R_{\rm pen} - \mu R_{\rm var} - \rho R_{\rm speed} + \gamma R_\Phi$, which is to be maximized, is concave if R_Φ is concave. We will come back to this shortly.

Many of the constraints are immediately convex. For example, limits on the quantities above are simple linear inequality constraints. The charge state dynamics, $\dot{Q}(t) = P_{\rm chg}(t) - \eta_{\rm loss}\,|P_{\rm chg}(t)|$, is a linear differential equation. We now turn to the other constraints, and show how they can be expressed as convex constraints on the variables listed above.

We can express the dynamics in terms of the kinetic energy as

$$\dot{K}(t) = J\omega_{\rm g}(t)\dot{\omega}_{\rm g}(t) = \omega_{\rm g}(t)\left(\frac{T_{\rm r}(t)}{N} - T_{\rm g}(t)\right) = P_{\rm w}(t) - P_{\rm g}(t)/\eta_{\rm g},$$

which is a linear differential equation relating K, $P_{\rm w}$, and $P_{\rm g}(t)$. The limits on rotor speed can be expressed as limits on kinetic energy, as

$$(J/2)\omega_{\rm g,min}^2 \leq K(t) \leq (J/2)\omega_{\rm g,max}^2.$$

These are simple linear (convex) inequalities.

The generator torque is

$$T_{\rm g}(t) = \frac{P_{\rm g}(t)}{\eta_{\rm g}\sqrt{(2/J)K(t)}}$$

(which shows how we can reconstruct it from the variables above), so the generator torque constraints translate into

$$0 \leq P_{\rm g}(t) \leq \eta_{\rm g}\sqrt{(2/J)K(t)}T_{\rm g,max},$$

which is a convex constraint on $P_{\rm g}(t)$ and $K(t)$, since $\sqrt{(2/J)K(t)}$ is a concave function of $K(t)$.

Finally, we explain how to reconstruct the blade pitch $\beta(t)$ from the variables listed above. We define the available wind power, as a function of wind speed and kinetic energy,

$$P_{\rm av}(v, K) = \max_{\beta_{\min} \leq \beta \leq \beta_{\max}} \Phi(v, (1/N)\sqrt{(2/J)K}, \beta)v^3.$$

This function is readily found (or tabulated in lookup table form) from Φ. By definition, we have

$$P_{\rm w}(t) \leq P_{\rm av}(v(t), K(t)), \tag{3}$$

which states that the extracted wind power cannot exceed the maximum available power.

Now we use a property of the function Φ: As β varies over its range, the extracted power varies from 0 to $P_{\rm av}$. In other words, by blade pitch control, we can vary the extracted power from 0 up to the maximum available power. We disregard the effects of dynamic inflow of the wind during fast pitching events, described in, *e.g.*, [52, 53, 54]. In these papers, the transient time of the dynamic inflow is observed to be in the range of 8-20 s. Thus, with a sample rate of 10 s, such effects are not relevant to this study. We define the function $\Psi(v, K, P_{\rm w})$ as the value of β that gives the extracted power $P_{\rm w}$. (This is how we will extract the blade pitch angle from the variables above.)

Now finally we turn to convexity of the constraint (3) and concavity of the objective term R_Φ. The latter readily translates into

$$R_\Phi = \int_0^T P_{\rm av}(v(t), K(t))\, dt.$$

What is needed to satisfy both is that, for each wind speed v, $P_{\rm av}$ is a concave function of K. Amazingly, this is the case with realistic coefficient of power models. (This is discussed below in §3.1.)

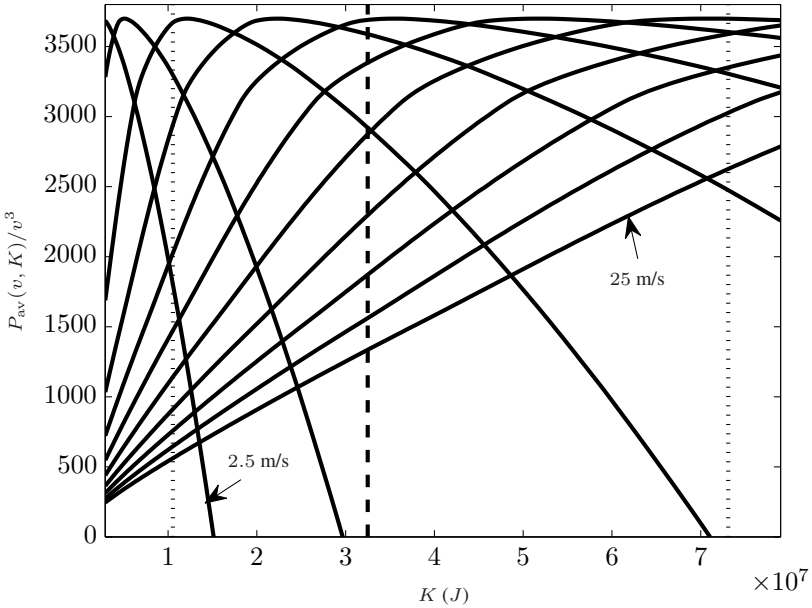

Figure 1. $P_{\mathrm{av}}(v, K)$ normalized by v^3 plotted for a number of different wind speeds evenly distributed between 2.5m/s and 25m/s. The dotted vertical lines show the minimum and maximum speeds and the dashed vertical line is the rated speed.

3.1. Concavity of the available power function

The concavity of the available power $P_{\mathrm{av}}(v, K)$ is not a mathematical fact. However, as we illustrate in Figure 1, the available power is nearly a concave function of K for each wind speed. Consequently, we can approximate each of these with a concave function which is very accurate. Let, $\hat{P}_{\mathrm{av},v_i}(K)$ be the approximation of $P_{\mathrm{av}}(v, K)$ (concave of K) at the wind speed v_i. We fit piecewise linear (PWL) functions to express this as

$$\hat{P}_{\mathrm{av},v_i}(K(t)) = \min\left\{a_1 K(t) + b_1, \ldots, a_k K(t) + b_k\right\} v^3,$$

with k affine functions (see, *e.g.*, [55]). We compute $\hat{P}_{\mathrm{av},v_i}(K)$ for a number of discrete values v_i of the wind speed.

For any given wind speed, we find the concave approximation $\hat{P}_{\mathrm{av}}(v, K)$ of the available power $P_{\mathrm{av}}(v, K)$ by linear interpolation of the two neighboring functions $\hat{P}_{\mathrm{av},v_i}(K)$, *e.g.*,

$$\hat{P}_{\mathrm{av}}(v(t), K(t)) = (1-\Theta)\hat{P}_{\mathrm{av},v_1}(K(t)) + \Theta\hat{P}_{\mathrm{av},v_2}(K(t)),$$

with $\Theta = \frac{v(t)-v_1}{v_2-v_1}$. $\hat{P}_{\mathrm{av}}(v, K)$ is a concave function of K as it is the linear interpolation of concave functions.

We validate the approximation by showing the error in $\hat{P}_{\mathrm{av}}(v, K)$ vs. $P_{\mathrm{av}}(v, K)$ for the valid range of v and K. We test with much smaller steps in v than what we have used for the PWL functions. See Figure 2. Our simple interpolated PWL fit has maximum error of a few percent, and typical error well under one percent.

4. NUMERICAL SIMULATION

We provide careful numerical simulations using the parameters for the NREL 5MW wind turbine model. The model is openly available and is described in detail in, *e.g.*, [56, 57]. For this turbine, the rated power is $P_{\mathrm{rated}} = 5$ MW which is reached at wind speeds above 11.4 m/s. The turbine cuts in at 3 m/s and out at 25 m/s. In this and in the following section, we present simulation results as normalized values using the per unit (pu) system throughout. We define this in Table I.

We solve the optimal control problem for a single turbine using our convex formulation:

$$\begin{array}{ll} \text{maximize} & E - \lambda R_{\mathrm{pen}} - \mu R_{\mathrm{var}} - \rho R_{\mathrm{speed}} + \gamma R_{\Phi}, \\ \text{subject to} & \text{constraints and dynamics given in } \S 3, \end{array} \tag{4}$$

where the variables are P_{g}, P_{grid}, P_{chg}, P_{w}, Q, and K (all functions of time). The optimization uses an initial state of the dynamic variables $K(t)$ and $Q(t)$ as well as known wind speeds for the interval. Instead of (4) we solve a discretized version with N_{p} steps over the time interval $[0, T]$ using the sample time T_{s}.

Wind Energ. 2013; **00**:1–12 © 2013 John Wiley & Sons, Ltd.
DOI: 10.1002/we
Prepared using weauth.cls

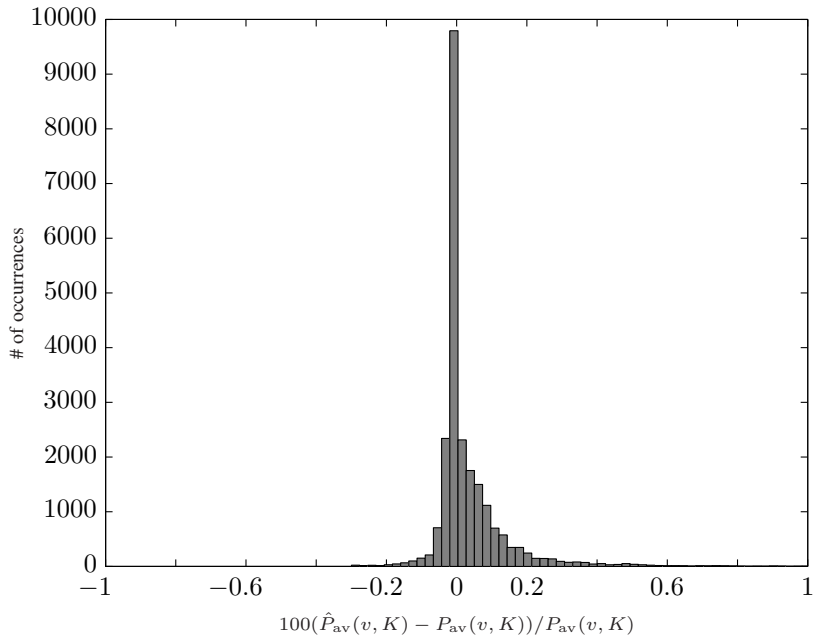

Figure 2. $\hat{P}_{\mathrm{av}}(v,K)$ error in percentage.

QUANTITY	FACTOR	INTERPRETATION
Power P	$1/P_{\mathrm{rated}}$	1 pu = rated turbine power
Kinetic energy K	$1/K_{\mathrm{rated}}$	1 pu = kinetic energy at rated speed
Storage capacity Q	$1/P_{\mathrm{rated}}$	1 pu = energy produced by the turbine at rated power in 1 s
Speed ω_{g}	$1/\omega_{\mathrm{g,rated}}$	1 pu = rated generator speed

Table I. Nomenclature for the pu system.

λ	$1 \cdot 10^{2}$	
μ	$1 \cdot 10^{-5}$	
ρ	$1 \cdot 10^{-2}$	
γ	$1 \cdot 10^{-2}$	
N_{p}	200	
T_{s}	10	s
η_{loss}	2	%
G	2.5	kW/s

Table II. Parameters for numerical simulation.

In addition to the parameters given by the model, we must choose values for the introduced dimensionless tuning parameters, for the target maximum value of power rate of change, for the charge/discharge loss, the sample time and the length of the interval. We let the maximum power gradient G be rather tight by allowing only a rate of change less than 3% of the maximum rated power per minute. We choose λ sufficiently high to enforce this maximum power gradient whenever possible. We want μ, ρ, and γ to be as small as possible and we adjust these by trial and error to give the desired behavior, *i.e.*, infrequent violation of the power gradient constraint, little variation in the power output, and limited use of overspeed. The method seems to be quite robust to changes in these values as the performance is merely dependent on the mutual relative size of the parameters. In this study we use a charge/discharge loss which is almost neglectable but still sufficient to avoid excessive charging and discharging over the interval. Table II gives the values used in the simulation. To put the kinetic energy in the rotational motion into play we allow over-speed up to 150% of the rated speed. The objective term R_{speed} keeps the turbine from over-speed when running in steady-state operation. The maximum storage capacity is varied in order to produce the trade-off plot in Figure 4. We formulate and solve this problem using CVX [58, 59].

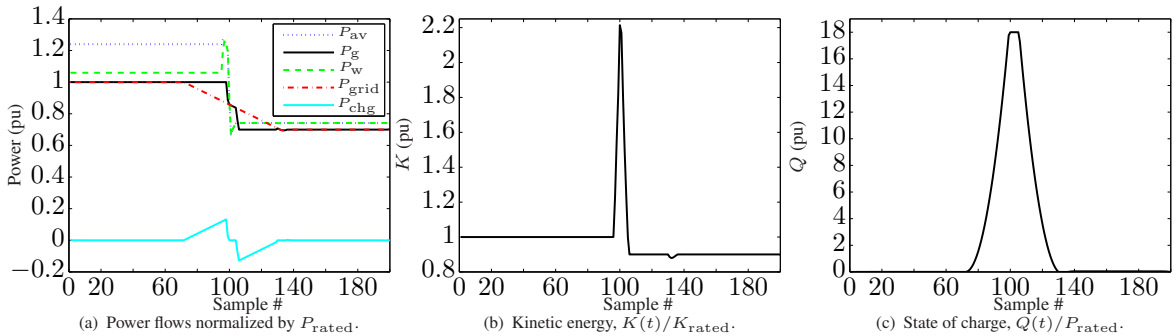

(a) Power flows normalized by $P_{\rm rated}$. (b) Kinetic energy, $K(t)/K_{\rm rated}$. (c) State of charge, $Q(t)/P_{\rm rated}$.

Figure 3. Test of power gradient satisfaction with open-loop optimization using perfect knowledge. We use pu as the unit for all quantities and let the wind speed drop from 12 m/s to 10 m/s linearly from sample 99 to 101. Note how the power signal decays before the drop in wind speed. Due to the predicted drop in available power the controller prepares for this in advance

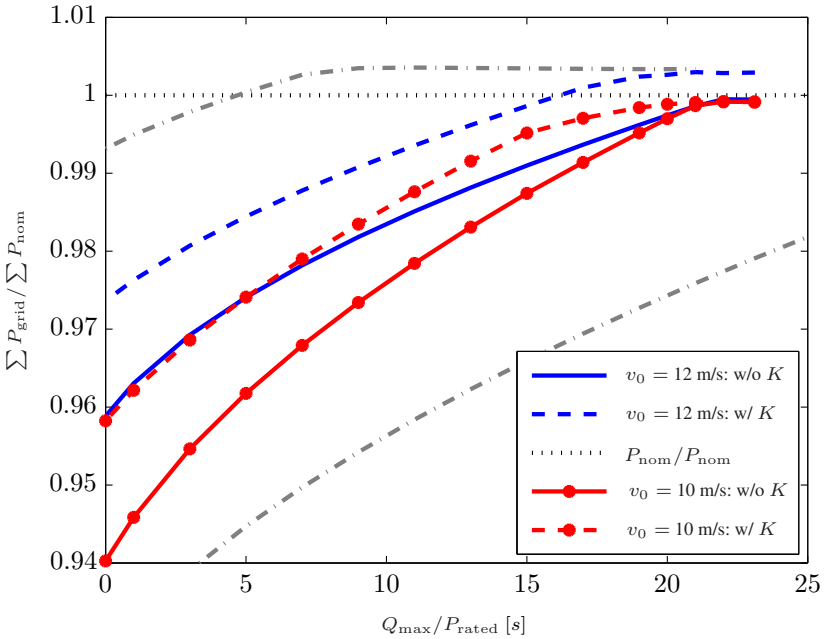

Figure 4. Energy delivered to the grid for varying storage capacity. We show two cases with a power drop of 0.3 pu over 20 s starting from v_0 above rated speed and below rated speed, respectively. We show this with and without kinetic energy storage K. The two grey dash-dot lines illustrate the dependency on the enforced power gradient as the upper curve comes from doubling the allowed gradient (loosening the constraint) while the lower curve is the result of allowing only half the power gradient (tightening the constraint). Both curves correspond to the $v_0 = 12$ m/s: w/ K curve (dashed blue). The lower curve reaches 1 at a storage level of approx. 40 pu.

Figure 3 shows the output from the optimizer for a selected scenario where the wind speed drops from 12 m/s to 10 m/s over a period of 20 s (2 samples). This equals a drop in available power (given in per unit (pu), *i.e.*, normalized by $P_{\rm rated}$) from around 1.2 pu to 0.7 pu. $Q_{\rm max}$ is 18 pu in this case. The difference between $P_{\rm w}$ and $P_{\rm g}$ that is noted in the figure in steady operation is due to the generator efficiency.

Figure 4 shows the accumulated power delivered to the grid over the interval as a function of available storage capacity. We demonstrate a drop in available power of 0.3 pu over 20 s for two different cases. One where the initial wind speed contains more power than $P_{\rm rated}$ and one where the available power is below $P_{\rm rated}$ for the entire interval. The figure shows both cases with and without the use of rotor inertia as additional energy storage. From Figure 4 we see how the active use of rotor inertia as energy storage can reduce the needed extra storage capacity by up to 30% without reducing the power output (when the initial wind speed is above rated). When no extra storage is available the power output can be increased around 2% in both cases by use of kinetic energy storage. In addition, Figure 4 can be used to evaluate the efficiency (in per cent of available wind power) of applying different amounts of external storage. In this case, the power gradient constraint is considered as hard, *i.e.*, something that must be fulfilled.

Wind Energ. 2013; **00**:1–12 © 2013 John Wiley & Sons, Ltd.
DOI: 10.1002/we
Prepared using weauth.cls

SCENARIO #	1	b	2	2b	3	3b	
Mean wind, $\bar{v}$	8.03	-	9.92/8.26	-	13.96/11.19	-	m/s
Max wind, $\max(v)$	9.88	-	12.31/9.47	-	15.59/13.18	-	m/s
Nominal vs. MPC, ΔP_{grid}	0.57	4.79	0.42	10.75	-0.93	2.97	%
Accumulated charge/discharge loss	0.21	-	0.23	-	0.04	-	%
Max storage, $Q_{\max}$	15.34	-	50	-	31.86	-	pu
Mean storage, $\bar{Q}$	5.45	-	16.60	-	8.31	-	pu
Max speed $\frac{\max(w_{\text{g}})}{w_{\text{g,rated}}}$	0.95	0.95	1.43	1.00	1.36	1.00	pu
Mean speed $\frac{\bar{w}_{\text{g}}}{w_{\text{g,rated}}}$	0.77	0.79	0.89	0.83	0.99	0.95	pu
Gradient violation time	1.05	21.15	1.54	28.04	1.27	14.41	%

Table III. Selected figures from the three closed-loop simulations. For scenario 2 and 3, the wind speed is given separately for the intervals before and after the drop in mean wind speed. To compare the performance of the controllers, ΔP_{grid} gives the difference in total delivered energy to the grid in per cent $100\frac{\sum P_{\text{grid,nominal}} - \sum P_{\text{grid,MPC}}}{\sum P_{\text{grid,nominal}}}$. For each scenario, the column denoted with 'b' provides the lost energy and the amount of power gradient violations for the same scenario but without the extra storage and overspeed capabilities.

5. MODEL PREDICTIVE CONTROL

In this section, we show simulations with real wind data series measured at the Danish wind turbine test site Høvsøre in 2004. The controller bases its decisions on a prediction of future wind speeds. We use the predictions generated in [60, 61] by modern continuous time formulations of the predictors together with spline basis expansions. The predictors use upstream wind speed information from other turbines or measurements located several hundred meters in front of the turbine. For the simulations in this section, we implement an economic optimizing model predictive controller to address the closed-loop control of a single wind turbine. Like in traditional MPC, we implement the controller in a receding horizon manner, where an optimization problem over N time steps (the control and prediction horizon) is solved at each step. The result is an optimal input sequence for the entire horizon, out of which only the first step is implemented. Our controller repeatedly solves the optimal control problem in (4). Consequently, the aim is to maximize the power delivered to the grid while obeying the strict requirements to power gradient constraints. This objective function relates to maximizing the profit within the limits of mechanical as well as regulated constraints, and we do not focus on tracking certain set-points as tend to be the trend in standard MPC.

We use the parameters for the optimal control problem given in Table II and present three different wind scenarios. Each scenario contains a number of 10-second averages of measured wind speed and their corresponding predictions. Scenario 1 covers 86 minutes with a quite constant mean wind speed while both scenario 2 and 3 show examples of significant drops in mean wind speed. Scenario 2 and 3 cover 215 minutes and 175 minutes, respectively. Figures 5–7 illustrate the wind scenario (measurement and prediction), the wind speed prediction error, power delivered to the grid, and the distribution of power gradients for each of the three scenarios. In each case, we compare our controller to the nominal controller in the full Simulink model for the NREL 5MW wind turbine [56, 57]. This turbine delivers all the power it produces directly to the grid and the pitch and generator torque control is based on gain-scheduled PI controllers that track optimal set-points given as look-up tables. This approach is standard in controlling wind turbines today. In addition to the figures, Table III provides a summary of interesting results from the simulations.

In all three scenarios, we note how the heavy fluctuations in power delivered to the grid almost disappear with our MPC controller. We see a much smoother power signal which is supported by the histograms that clearly show how the rate of change of the power (with a few exceptions) is limited to the $\pm 3\%$/minute range that we allow in the problem formulation. For scenario 1 and 2 the total amount of energy delivered to the grid is reduced by 0.57% and 0.42%, respectively. This reduction is due to a total accumulated charge/discharge loss of around 0.2% and some periods with suboptimal operation since we change the rotor speed. Note that this lost energy production should be seen in relation to the much higher losses incurred when no storage is available (columns denoted 'b' in Table III), as the power gradient is regarded as a strictly enforced grid code. In scenario 3, the wind speed is above the rated speed most of the time and our MPC controller increases the amount of energy delivered to the grid in this case. This increase comes from the improved power coefficient during overspeed. Table III provide further results regarding maximum and mean utilization of external storage capacity, maximum and mean rotor speed, etc.

6. CONCLUSION

In this paper, we have presented an approach to power gradient reduction for fulfilling future, tighter grid codes and for improving the quality of power delivered to the grid from wind power plants. We utilize turbine inertia as a resource of distributed energy storage, limited by the rotational speed, in addition to a central storage unit which is associated with an extra cost. We have demonstrated that by a novel change of variables we can transform the quite nonlinear system dynamics to a model with linear dynamics and convex constraints. Thus, the problem can be solved for its global optimum using very efficient and reliable algorithms. Simulations on realistic models reveal a significant ability to reject the disturbances from fast changes in wind speed, ensuring certain power gradients, while keeping the amount of produced power very close to nominal.

ACKNOWLEDGEMENTS

We thank Lars Finn Sloth Larsen, Martin Ansbjerg Kjær, Germán Claudio Tarnowski, and Richard Powers from Vestas Technology R&D for helpful discussions, ideas and suggestions. Furthermore, we thank Henrik Aalborg Nielsen from Enfor A/S, Henrik Madsen from DTU Compute, and Poul Sørensen from DTU Wind Energy for access to the real wind data and their predictions as well as for helpful suggestions on wind forecasting methods.

REFERENCES

1. Danish Ministry of Climate E, Building. Energy policy report 2012. http://www.ens.dk/en-US/policy/danish-climate-and-energy-policy/Sider/danish-climate-and-energy-policy.aspx 2012.
2. Morren J, Pierik J, de Haan SWH. Inertial response of variable speed wind turbines. *Electric Power Systems Research* 2006; **76**(11):980–987.
3. Conroy JF, Watson R. Frequency Response Capability of Full Converter Wind Turbine Generators in Comparison to Conventional Generation. *IEEE Transactions on Power Systems* 2008; **23**(2):649–656.
4. Iov F, Hansen A, Sørensen P, Cutululis N. A survey of interconnection requirements for wind power. *Proc. of the Nordic wind power conference (NWPC)*, Risø National Laboratory, 2007.
5. Singh B, Singh S. Wind Power Interconnection into the Power System: A Review of Grid Code Requirements. *The Electricity Journal* 2009; **22**(5):54–63.
6. Eltra/Elkraft/Energinetdk. Regulation TF 3.2.5, Wind turbines connected to grids with voltages above 100 kV — Technical regulation for the properties and the regulation of wind turbines. https://selvbetjening.preprod.energinet.dk/NR/rdonlyres/E4E7A0BA-884F-4E63-A2F0-98EB5BD8D4B4/0/WindTurbinesConnectedtoGridswithVoltageabove100kV.pdf 2004.
7. ENTSO-E. Network code for requirements for grid connection applicable to all generators. https://www.entsoe.eu/fileadmin/user_upload/_library/consultations/Network_Code_RfG/120626_final_Network_Code_on_Requirements_for_Grid_Connection_applicable_to_all_Generators.pdf 2012.
8. Korpås M, Holen AT. Operation planning of hydrogen storage connected to wind power operating in a power market. *IEEE Transactions on Energy Conversion* 2006; **21**(3):742–749.
9. Black M, Strbac G. Value of Bulk Energy Storage for Managing Wind Power Fluctuations. *IEEE Transactions on Energy Conversion* 2007; **22**(1):197–205.
10. Stroe DI, Stan AI, Diosi R, Teodorescu R, Andreasen SJ. Short term energy storage for grid support in wind power applications. *Proc. of the 13th International Conference on Optimization of Electrical and Electronic Equipment (OPTIM)*, 2012; 1012–1021.
11. Budischak C, Sewell DA, Thomson H, Mach L, Veron DE, Kempton W. Cost-Minimized Combinations of Wind Power, Solar Power and Electrochemical Storage, Powering the Grid up to 99.9% of the Time. *Journal of Power Sources* 2013; **225**:60–74.
12. Swierczynski M, Teodorescu R, Rodriguez P. Lifetime investigations of a lithium iron phosphate (LFP) battery system connected to a wind turbine for forecast improvement and output power gradient reduction. *Proc. of the 15th Battcon Stationary Battery Conference and Trade Show*, 2011; 20.1–20.8.
13. Hovgaard TG, Larsen LFS, Edlund K, Jørgensen JB. Model predictive control technologies for efficient and flexible power consumption in refrigeration systems. *Energy* 2012; **44**(1):105 – 116.
14. Hovgaard TG, Larsen LFS, Jørgensen JB, Boyd S. Nonconvex model predictive control for commercial refrigeration. *International Journal of Control* 2013; **86**(8):1349 – 1366.

15. Knuppel T, Nielsen JN, Jensen KH, Dixon A, Østergaard J. Power oscillation damping controller for wind power plant utilizing wind turbine inertia as energy storage. *Proc. of the IEEE Power and Energy Society General Meeting*, 2011; 1–8.
16. Tarnowski GC. Coordinated Frequency Control of Wind Turbines in Power Systems with High Wind Power Penetration. PhD Thesis, Technical University of Denmark 2012.
17. Hau E. *Wind turbines: fundamentals, technologies, application, economics*. Springer Verlag, 2006.
18. Hammerum K, Brath P, Poulsen NK. A fatigue approach to wind turbine control. *Journal of Physics: Conference Series* 2007; **75**.
19. Dang DQ, Wu S, Wang Y, Cai W. Model Predictive Control for maximum power capture of variable speed wind turbines. *International Power Electronics Conference*, 2010; 274–279.
20. Henriksen LC, Poulsen NK, Hansen MH. Nonlinear Model Predictive Control of a Simplified Wind Turbine. *Proc. of the 18th IFAC World Congress*, 2011; 551–556.
21. Adegas FD, Stoustrup J, Odgaard PF. Repetitive model predictive approach to individual pitch control of wind turbines. *Proc. of the IEEE Conference on Decision and Control*, 2011; 3664–3670.
22. Hansen AD, Sørensen P, Iov F, Blaabjerg F. Centralised power control of wind farm with doubly fed induction generators. *Renewable Energy* 2006; **31**(7):935–951.
23. Spudic V, Jelavic M, Baotic M. Wind turbine power references in coordinated control of wind farms. *AUTOMATIKA* 2011; **52**(2):82–94.
24. Madjidian D, Rantzer A. A Stationary Turbine Interaction Model for Control of Wind Farms. *Proc. of the 18th IFAC World Congress*, 2011; 4921–4926.
25. Soleimanzadeh M, Wisniewski R, Kanev S. An optimization framework for load and power distribution in wind farms. *Journal of Wind Engineering and Industrial Aerodynamics* 2012; **107–108**:256–262.
26. Hovgaard TG, Larsen LFS, Jørgensen JB, Boyd S. Sequential Convex Programming for Power Set-point Optimization in a Wind Farm using Black-box Models, Simple Turbine Interactions, and Integer Variables. *Proc. of the 10th European Workshop on Advanced Control and Diagnosis (ACD)*, 2012; 1–8.
27. Hovgaard TG, Larsen LFS, Jørgensen JB, Boyd S. MPC for Wind Power Gradients Utilizing Forecasts, Rotor Inertia, and Central Energy Storage. *Proc. of the European Control Conference*, 2013; 4071–4076.
28. Garcia CE, Prett DM, Morari M. Model predictive control: theory and practice-a survey. *Automatica* 1989; **25**(3):335–348.
29. Bemporad A, Morari M. Robust model predictive control: A survey. *Robustness in Identification and Control* 1999; :207–226.
30. Qin SJ, Badgwell TA. A survey of industrial model predictive control technology. *Control engineering practice* 2003; **11**(7):733–764.
31. Rawlings JB, Amrit R. Optimizing Process Economic Performance Using Model Predictive Control. *Nonlinear Model Predictive Control: Towards New Challenging Applications* 2009; :119–138.
32. Diehl M, Amrit R, Rawlings JB. A Lyapunov Function for Economic Optimizing Model Predictive Control. *Automatic Control, IEEE Transactions on* 2011; **56**(3):703–707.
33. Angeli D, Amrit R, Rawlings J. On average performance and stability of Economic Model Predictive Control. *Automatic Control, IEEE Transactions on* 2012; **57**(7):1615–1626.
34. Rawlings JB, Angeli D, Bates C. Fundamentals of economic model predictive control. *Proc. of the 51th IEEE Conference on Decision and Control*, 2012; 3851–3861.
35. Grüne L. Economic receding horizon control without terminal constraints. *Automatica* 2013; **49**(3):725–734.
36. Halvgaard R, Poulsen NK, Madsen H, Jørgensen JB. Economic Model Predictive Control for building climate control in a Smart Grid. *Innovative Smart Grid Technologies (ISGT), 2012 IEEE PES*, 2012; 1–6.
37. Oldewurtel F, Parisio A, Jones CN, Gyalistras D, Gwerder M, Stauch V, Lehmann B, Morari M. Use of model predictive control and weather forecasts for energy efficient building climate control. *Energy and Buildings* 2012; **45**(0):15–27.
38. Mirzaei M, Poulsen NK, Niemann HH. Robust Model Predictive Control of a Wind Turbine. *Proc. of the 2012 American Control Conference*, 2012; 4393–4398.
39. Henriksen LC, Hansen MH, Poulsen NK. Wind turbine control with constraint handling: a model predictive control approach. *I E T Control Theory and Applications* 2012; **6**(11):1722–1734.
40. Biegel B, Juelsgaard M, Kraning M, Boyd S, Stoustrup J. Wind turbine pitch optimization. *IEEE International Conference on Control Applications (CCA)*, 2011; 1327–1334.
41. Soltani M, Wisniewski R, Brath P, Boyd S. Load reduction of wind turbines using receding horizon control. *IEEE International Conference on Control Applications (CCA)* , 2011; 852–857.
42. Kraning M, Wang Y, Akuiyibo E, Boyd S. Operation and Configuration of a Storage Portfolio via Convex Optimization. *Proc. of the 18th IFAC World Congress*, 2011; 10 487–10 492.

43. Kraning M, Chu E, Lavaei J, Boyd S. Dynamic Network Energy Management via Proximal Message Passing. *Foundations and Trends in Optimization* 2013; **1**(2):70–122.
44. Rao CV, Wright SJ, Rawlings JB. Application of interior-point methods to model predictive control. *Journal of optimization theory and applications* 1998; **99**(3):723–757.
45. Jørgensen JB. Moving Horizon Estimation and Control. PhD Thesis, Department of Chemical Engineering, Technical University of Denmark 2005.
46. Wang Y, Boyd S. Fast Model Predictive Control Using Online Optimization. *IEEE Transactions on Control Systems Technology* 2010; **18**(2):267–278.
47. Jørgensen JB, Frison G, Gade-Nielsen NF, Dammann B. Numerical methods for solution of the extended linear quadratic control problem. *Proc. of the 4th IFAC Nonlinear Model Predictive Control Conference*, 2012; 187–193.
48. Mattingley J, Boyd S. CVXGEN: a code generator for embedded convex optimization. *Optimization and Engineering* 2012; **13**:1–27.
49. Mattingley J, W Y, Boyd S. Receding Horizon Control. *IEEE Control Systems Magazine* 2011; **31**(3):52–65.
50. O'Donoghue B, Stathopoulos G, Boyd S. A Splitting Method for Optimal Control. *IEEE Transactions on Control Systems Technology* Nov 2013; **21**(6):2432–2442.
51. Boyd S, Vandenberghe L. *Convex Optimization*. Cambridge University Press, 2004.
52. Øye, S. Tjæreborg Wind Turbine. *AFM notat*, Department of fluid mechanics, DTU, Denmark., 1991.
53. Øye, S. Fast pitch step experiments in a wind tunnel and comparison with computational methods. *Proc. of the 1996 European Union Wind Energy Conference*, 1996; 741–744.
54. Knudsen, T and Bak, T. Simple model for describing and estimating wind turbine dynamic inflow. *Proc. of the American Control Conference (ACC)*, 2013; 640–646.
55. Magnani A, Boyd S. Convex piecewise-linear fitting. *Optimization and Engineering* 2009; **10**(1):1–17.
56. Jonkman JM, Butterfield S, Musial W, Scott G. *Definition of a 5-MW reference wind turbine for offshore system development*. National Renewable Energy Laboratory, 2009.
57. Grunnet JD, Soltani M, Knudsen T, Kragelund MN, Bak T. Aeolus Toolbox for Dynamics Wind Farm Model, Simulation and Control. *Proc. of the European Wind Energy Conference and Exhibition, EWEC*, 2010.
58. CVX Research I. CVX: Matlab Software for Disciplined Convex Programming, version 2.0 beta. http://cvxr.com/cvx 2012.
59. Grant M, Boyd S. Graph implementations for nonsmooth convex programs. *Recent Advances in Learning and Control*, V Blondel and S Boyd and H Kimura (ed.). Lecture Notes in Control and Information Sciences, Springer-Verlag Limited, 2008; 95–110.
60. Nielsen HA, Madsen H, Sørensen P. Ultra-short term wind speed forecasting. *Proc. of the European Wind Energy Conference & Exhibition, London*, 2004.
61. Nielsen HA, Madsen H. Forecasting wind speeds on the minute time-scale using up-stream information. *Technical Report*, Technical University of Denmark, Informatics and Mathematical Modelling 2004.

Wind Energ. 2013; **00**:1–12 © 2013 John Wiley & Sons, Ltd.
DOI: 10.1002/we
Prepared using weauth.cls

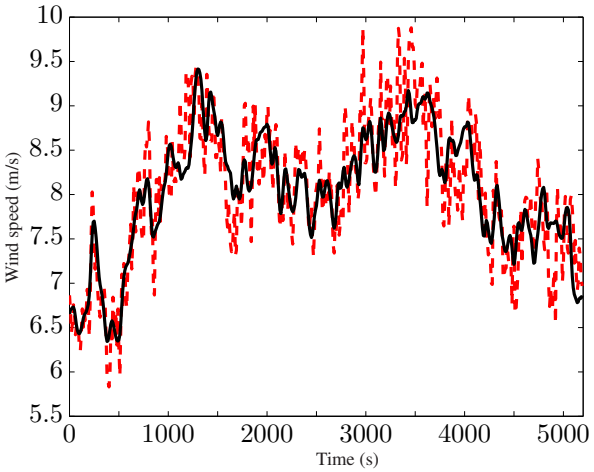

(a) Measured wind speed (dashed red) and predicted wind speed (solid black).

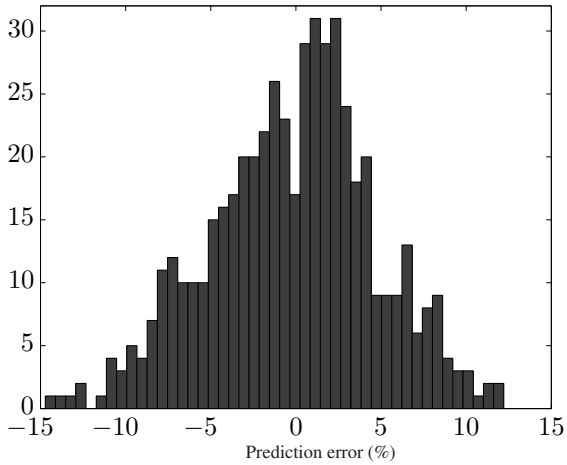

(b) Wind speed prediction error in per cent

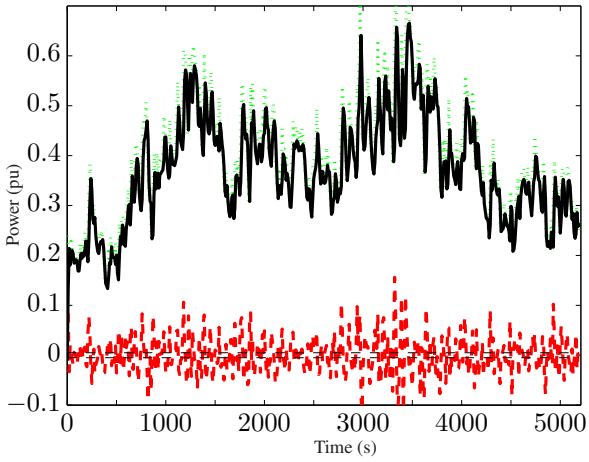

(c) Nominal controller: P_{grid} (solid black), $\max P_{\text{av}}$ (dotted green), and ΔP_{grid}/sample (dashed red).

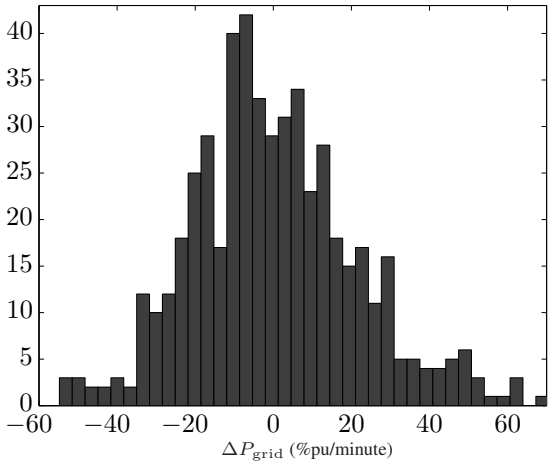

(d) Nominal controller: Power gradient in per cent of rated power per minute.

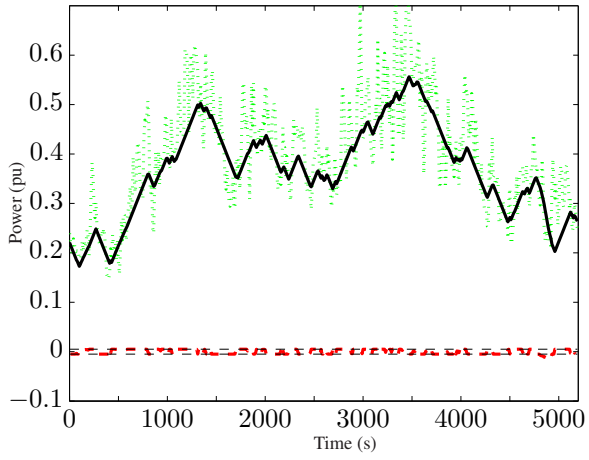

(e) MPC controller: P_{grid} (solid black), $\max P_{\text{av}}$ (dotted green), and ΔP_{grid}/sample (dashed red).

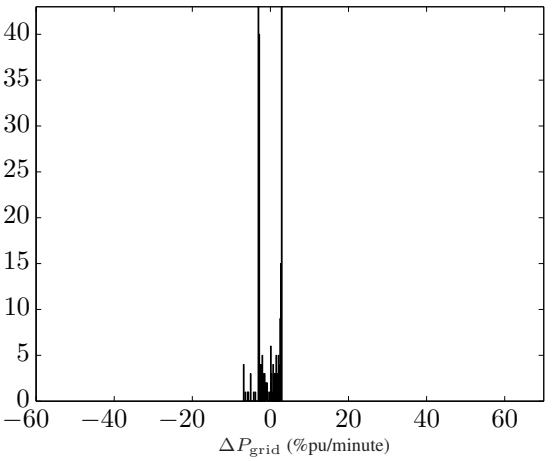

(f) MPC controller: Power gradient in per cent of rated power per minute.

Figure 5. Closed-loop simulation of MPC controller with wind scenario 1.

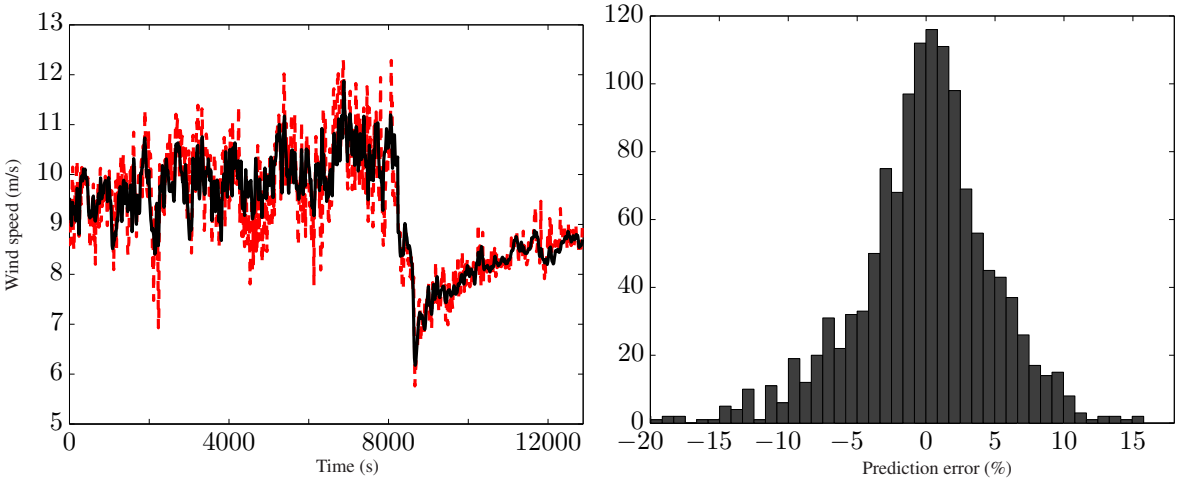

(a) Measured wind speed (dashed red) and predicted wind speed (solid black).

(b) Wind speed prediction error in per cent

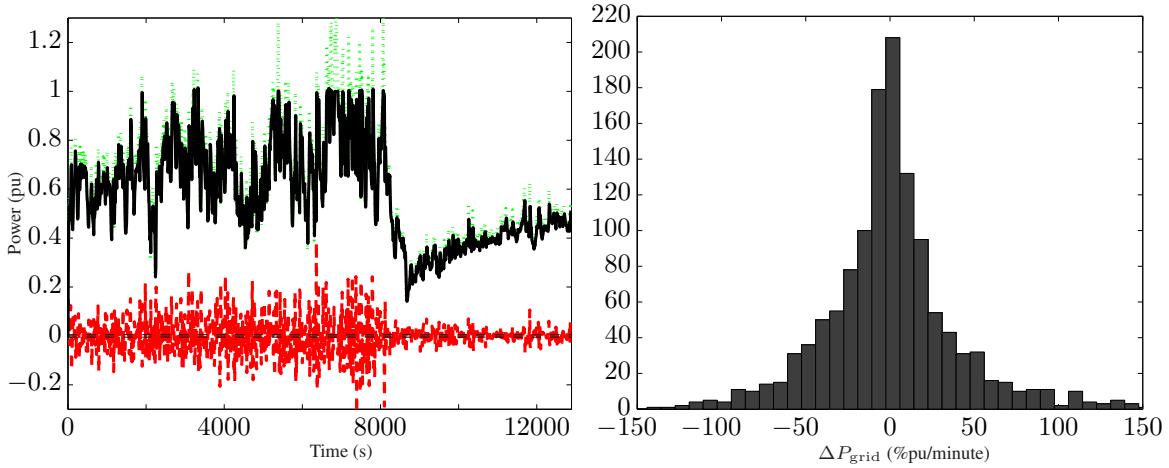

(c) Nominal controller: P_{grid} (solid black), $\max P_{\mathrm{av}}$ (dotted green), and ΔP_{grid}/sample (dashed red).

(d) Nominal controller: Power gradient in per cent of rated power per minute.

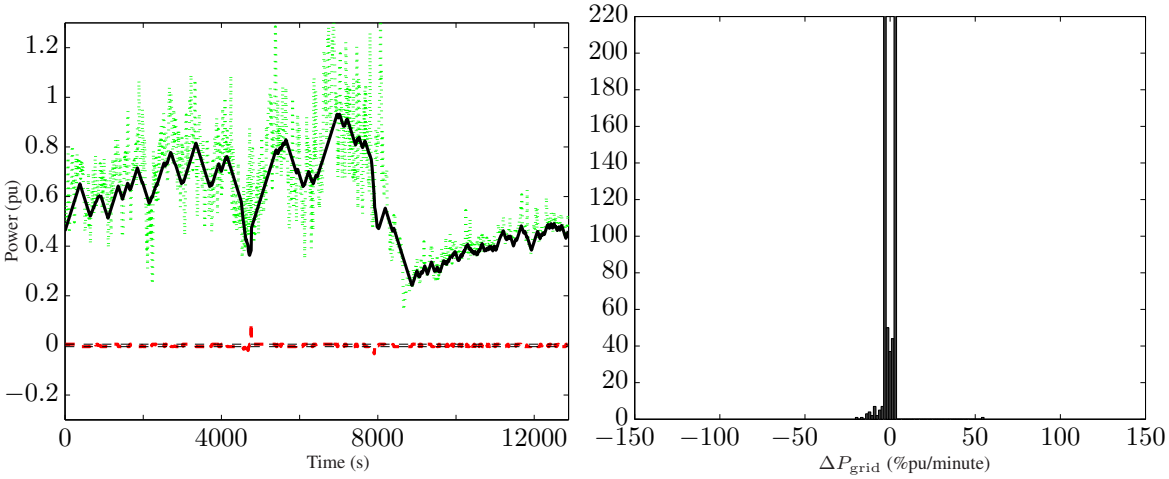

(e) MPC controller: P_{grid} (solid black), $\max P_{\mathrm{av}}$ (dotted green), and ΔP_{grid}/sample (dashed red).

(f) MPC controller: Power gradient in per cent of rated power per minute.

Figure 6. Closed-loop simulation of MPC controller with wind scenario 2.

Wind Energ. 2013; **00**:1–12 © 2013 John Wiley & Sons, Ltd.
DOI: 10.1002/we
Prepared using weauth.cls

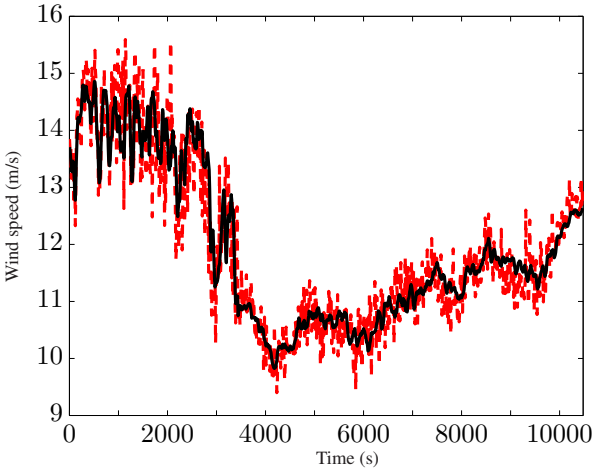

(a) Measured wind speed (dashed red) and predicted wind speed (solid black).

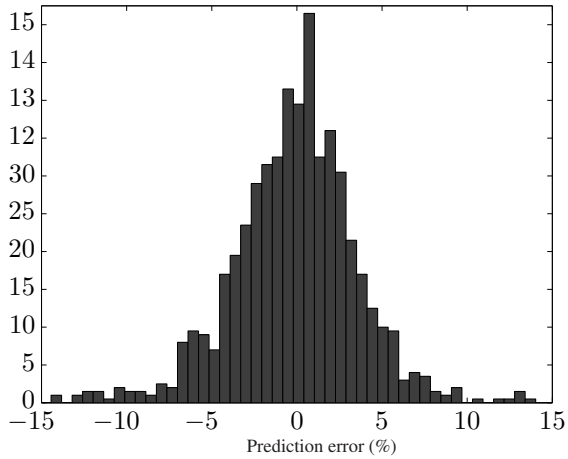

(b) Wind speed prediction error in per cent

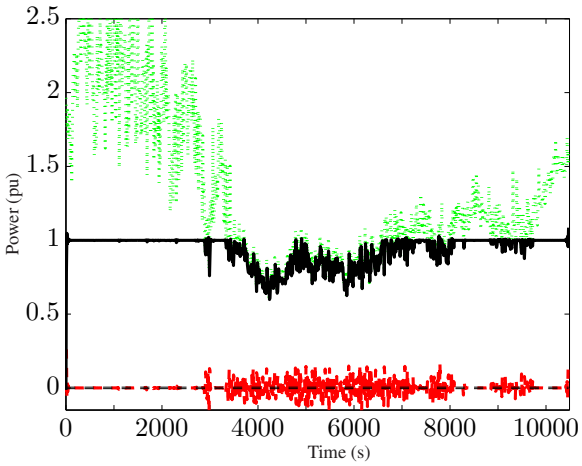

(c) Nominal controller: P_{grid} (solid black), $\max P_{\text{av}}$ (dotted green), and ΔP_{grid}/sample (dashed red).

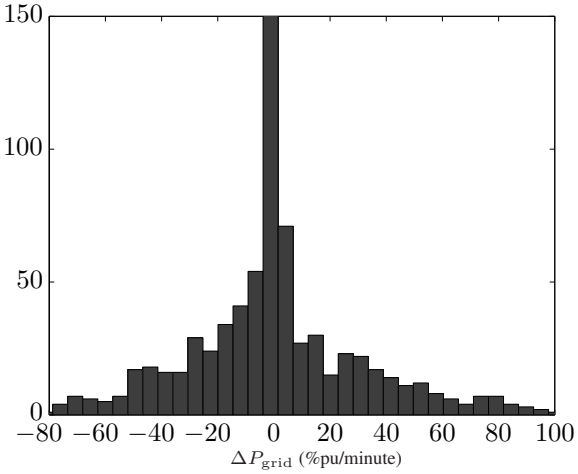

(d) Nominal controller: Power gradient in per cent of rated power per minute.

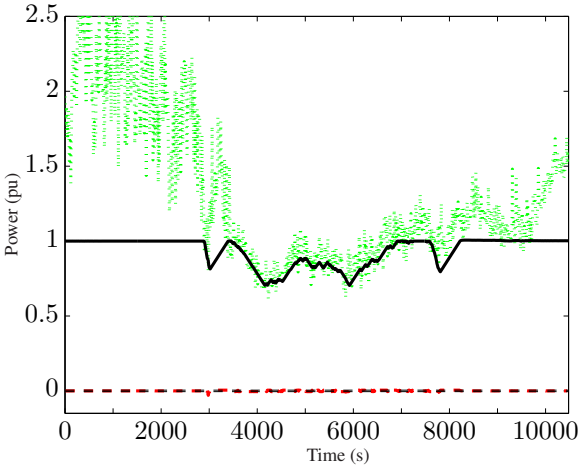

(e) MPC controller: P_{grid} (solid black), $\max P_{\text{av}}$ (dotted green), and ΔP_{grid}/sample (dashed red).

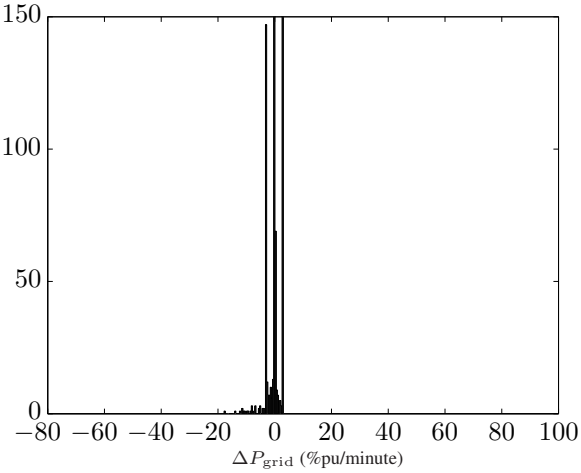

(f) MPC controller: Power gradient in per cent of rated power per minute.

Figure 7. Closed-loop simulation of MPC controller with wind scenario 3.